iJRASET
International Journal For Research in Applied Science and Engineering Technology

INTERNATIONAL JOURNAL FOR RESEARCH

IN APPLIED SCIENCE & ENGINEERING TECHNOLOGY

Volume: 3 **Issue:** VI **Month of publication:** June 2015

DOI:

www.ijraset.com

Call: 08813907089 | E-mail ID: ijraset@gmail.com

Volume 3 Issue VI, June 2015
ISSN: 2321-9653
International Journal for Research in Applied Science & Engineering Technology (IJRASET)

Performance Investigation of Hybrid Power System with Wind Energy Conversion System

Sona Mathew[1], Ajay Amrit Raj[2]
[1,2]M.E Power Systems Engineering, Anna University Chennai

***Abstract*—This paper presents the automatic reactive power control of isolated wind–diesel hybrid power systems having a permanent-magnet induction generator for a wind energy conver- sion system and a synchronous generator for a diesel generator set. To minimize the gap between reactive power generation and demand, a variable source of reactive power is used such as a static synchronous compensator. The mathematical model of the system used for simulation is based on small-signal analysis. Three examples of the wind–diesel hybrid power system are considered with different wind power generation capacities to study the effect of the wind power generation on the system performance. This paper also shows the dynamic performance of the hybrid system with and without change in input wind power plus 1% step increase in reactive power load.**
***Index Terms*- Permanent-magnet induction generator (IG) (PMIG), static synchronous compensator (STATCOM), synchro- nous generator (SG), wind–diesel hybrid system.**

I. INTRODUCTION

Large interconnected power systems provide power to the community at large for the optimum utilization of the available power sources. However, due to the non availability of sufficient funds, constraints on the right way of providing additional transmission lines and rapid growth in load result in unfulfilled demand, particularly in developing countries like India. Also, the gap between demand and supply is increasing day by day. To reduce the gap, the sources such as solar, wind, mini/micro hydro, biogas, etc. have been introduced extensively as nonconventional energy sources that also con-tribute to environmental protection, along with other alternative sources. Some of the communities/areas, where grid supply is not available, have been benefited by having these sources as a parallel operation with existing diesel generator units [1]–[8]. At present, the bulk of the power generated from wind, small hydro, etc. is pumped to the grid also. These systems are known as isolated hybrid power systems. The diesel engine with SG ac as an isolated grid and the operation of wind turbines with IGs are in parallel to meet the demand of the isolated community [9], [10]. However, the performance of an IG is poor in terms of voltage regulation as it requires a magnetizing current from the source for excitation [9], [11], [12]. This decreases both the power factor and efficiency of the IG [13].

The power factor, voltage regulation, and efficiency can be improved by the use of PMIG [13]. In PMIG, permanent magnets are incorporated in the conventional rotor of an IG. To analyze the steady-state performance of the PMIG, various models and their applications have been discussed in [13]– [20]. A *d–q* reference model for a PMIG has been described in [15]. The performance of the PMIG using an impedance model based on a conventional per-phase equivalent circuit with per- unit parameters has also been investigated in [13] and [16]. The modeling of PMIG is very important which can easily be extended for the multi machine systems as given in [19] and is considered in this paper. There may be balance in the generated and absorbed reactive power by the system having SG, IG/PMIG, and load.

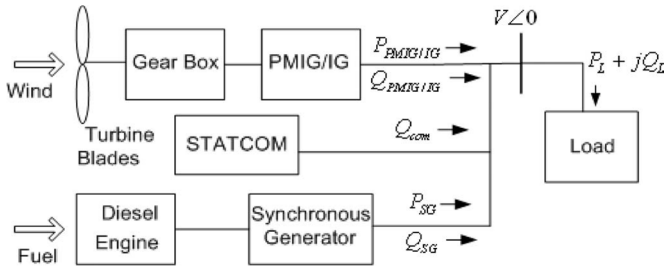

Fig. 1. Single line diagram of an isolated wind–diesel hybrid power system

The imbalance may cause severe problems in the system. Hence, a variable source of reactive power is required to eliminate

©IJRASET 2015: All Rights are Reserved

mismatch between the gen- eration and consumption of reactive power. Various flexible- ac-transmission-system devices, such as switched capacitors, static VAR compensator, and STATCOM, are available which can supply fast and continuous reactive power [21], [22]. The STATCOM [21]–[24] employing a voltage source converter (VSC) that internally generates inductive or capacitive reactive power as required is considered in this paper. The system state space model based on small signal is derived for an isolated wind–diesel system with STATCOM. Simulation studies of the system having different sizes of wind turbines with IG and PMIG are carried out. The integral square error (ISE) criterion is used to evaluate the optimum gain settings of the controller parameters of the STATCOM. Finally, the transient responses of the hybrid system are also shown both for IG and PMIG for the step increase in reactive power load (1% to 10%) with and without step change in input wind power.

II. MATHEMATICAL MODELING OF HYBRID POWER SYSTEM

A wind–diesel hybrid power system with STATCOM con- sidered for study is shown in Fig. 1. The real and reactive power balance equations of the system under steady-state conditions are

$$P_{PMIG/IG} + P_{SG} = P_L \quad (1)$$

$$Q_{SG} + Q_{COM} + Q_{PMIG} = Q_L \quad \ldots\ldots\ldots\ldots 2$$

Due to disturbance in load reactive power ΔQL, the system voltage may change which results in an incremental change in reactive power of other components. The net reactive power surplus is $\Delta QSG + \Delta Qcom + \Delta QPMIG/IG - \Delta QL$, and it will change the system bus voltage which will govern by the following transfer function equation:

$$\Delta V(s) = \frac{Kv}{1+sTv}[\Delta Q_{SG}(s) + \Delta Q_{com}(s) + \Delta Q_{PMIG}(s) - \Delta Q_L(s)] \quad \ldots\ldots 3$$

where *KV* and *TV* are the system gain and time constant, respectively. All the connected loads experience an increase with the increase in voltage due to load voltage characteristics
as shown in the following:

$$D_v = \frac{\partial Q_L}{\partial V} \quad \ldots\ldots 4$$

The composite loads can be expressed in exponential voltage form as

$$Q_L = c_1 V^q \quad \ldots\ldots 5$$

The load voltage characteristics *DV* can be found empirically as

$$D_V = \frac{\Delta Q_L}{\Delta V} = q.\frac{Q_L^0}{V^0} \quad \ldots\ldots\ldots\ldots 6$$

In (3), $KV = 1/DV$, and *TV* is the time constant of the system which is proportional to the ratio of the electromagnetic energy stored in the winding to the reactive power absorbed by the system. An IEEE type-1 excitation control system as shown in Fig. 2 is considered for the SG of the hybrid system with saturation neglected; therefore, the state transfer equations are

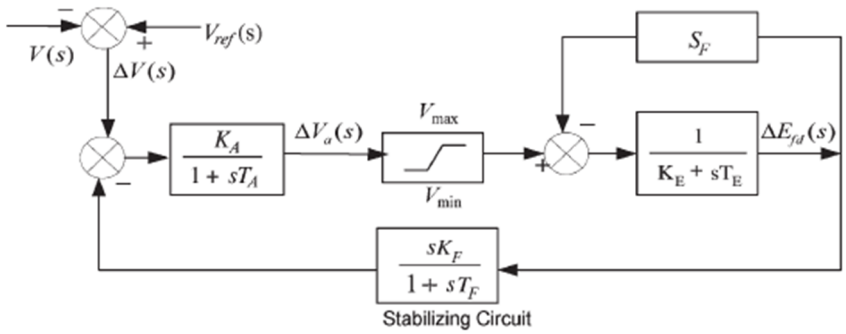

Fig .2. IEEE Type-1Excitation control system

©IJRASET 2015: All Rights are Reserved

Volume 3 Issue VI, June 2015
ISSN: 2321-9653
International Journal for Research in Applied Science & Engineering Technology (IJRASET)

$$\Delta E_{fd}(s) = \frac{1}{K_E + sT_E} \Delta V_{\alpha}(s) \text{.....7}$$

$$\Delta V_{\alpha}(s) = \frac{K_A}{1+sT_A} \left(\Delta V(s) - \frac{K_F}{T_F} \Delta E_{fd}(s) + \Delta V_f(s) \right) \text{.....8}$$

$$\Delta V_f(s) = \frac{K_F}{T_F} \frac{1}{1+sT_F} \Delta E_{fd}(s) \text{.....9}$$

The small change in voltage behind transient reactance $\Delta Eq(s)$ by solving the flux linkage equation for small perturbation is given as follows:

$$\Delta E'_q(s) = \frac{1}{1+sT_G} [K_1 \Delta E_{fd}(s) + K_2 \Delta V(s)] \text{.....10}$$

Where

$$K_1 = X'_d / X_d \; ; \quad K_2 = [(X'_d - X_d) \cos\delta] / X_d \text{ and}$$

$$T_G = T'_{do} X'_d / X_d$$

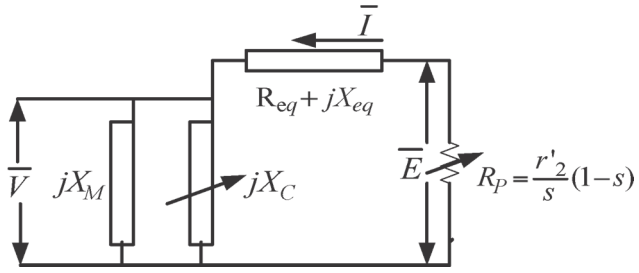

Fig. 3. Approximate equivalent circuit of PMIG

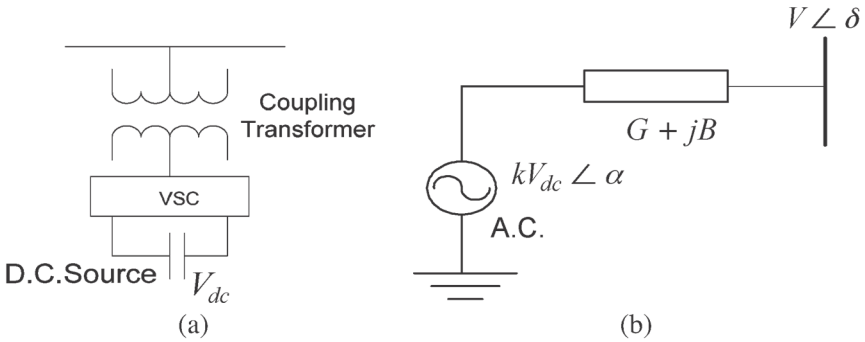

Fig. 4. STATCOM configuration: (a) Schematic diagram and (b) equivalent circuit

The small change in SG reactive power in terms of state variables is given by

$$\Delta Q_{SG}(s) = K_3 \Delta E'_q(s) + K_4 \Delta V(s) \text{.....11}$$

Optimum gain settings of STATCOM for different hybrid power systems
Where

©IJRASET 2015: All Rights are Reserved

Volume 3 Issue VI, June 2015
ISSN: 2321-9653
International Journal for Research in Applied Science & Engineering Technology (IJRASET)

$$K_3 = V \cos \partial / X'_d$$

$$K_4 = [E' \cos \partial - 2V] / X'_d$$

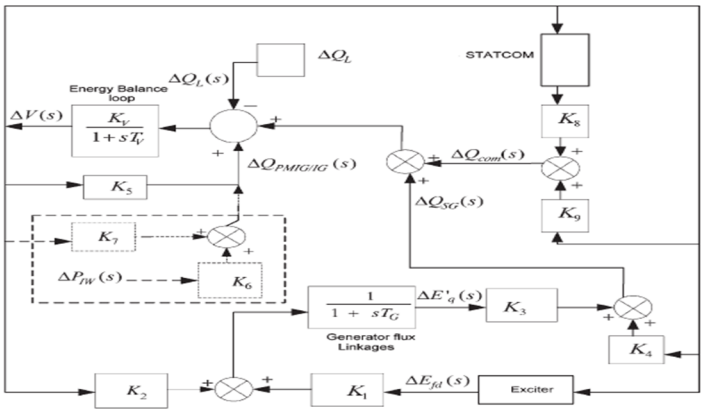

Fig 5. Transfer Function Block Diagram of the Wind-Diesel System

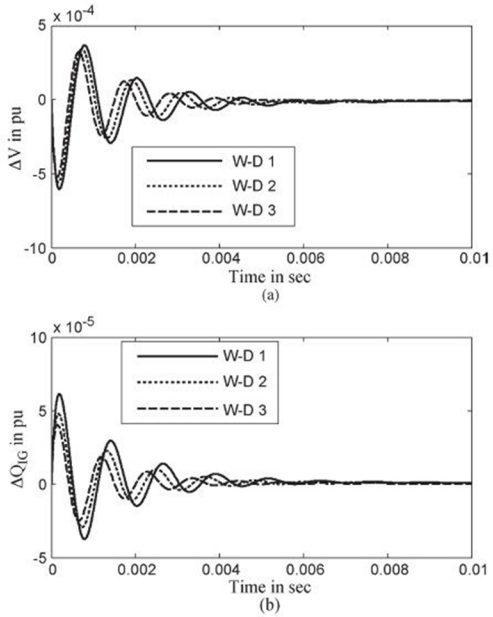

Fig. 6. Transient responses of the system (W-D with IG) for 1% step increase in load, with no change in input wind power

Wind-Diesel System Data(W-D)	Constant Slip		Variable Slip	
	K_P	K_I	K_P	K_I
W-D1	39	5090	31	5000
W-D2	53	6727	43	6636
W-D3	70	10899	68	10700
W-D1	37	6181	36	6000
W-D2	52	8363	51	8181
W-D3	68	14434	66	14242

TABLE 5.1

©IJRASET 2015: All Rights are Reserved

Volume 3 Issue VI, June 2015
ISSN: 2321-9653
International Journal for Research in Applied Science & Engineering Technology (IJRASET)

Equation (11) expresses $\Delta QSG(s)$ of (3) in terms of system state variables $\Delta Eq(s)$ and $\Delta V(s)$. Similarly, $\Delta QPMIG(s)$ can be expressed in terms of system state variables as given hereinafter. For small perturbations, the reactive power absorbed by PMIG, $\Delta QPMIG(s)$, in terms of generator terminal voltage and generator parameters can be written as:

$$\Delta Q_{PMIG}(s) = K_5 \Delta V(s) \text{.....(12)}$$

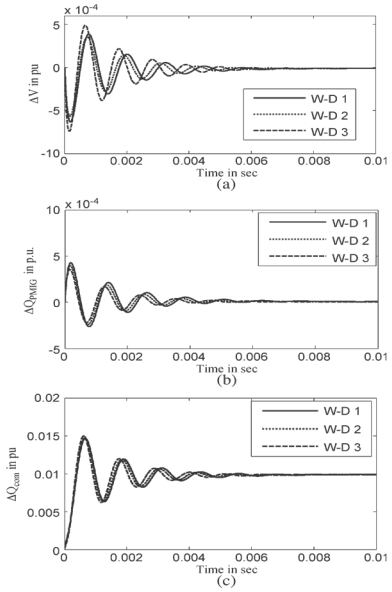

Fig. 7. Transient responses of the system (W-D with PMIG) for 1% step increase in load, with no change in input wind power

Where

$$K_5 = \frac{-2X_{eq}V}{R_T^{\,2} + X_{eq}^{\,2}} + \frac{V^2}{X_C}\left\{\frac{(3aV^2 + 2bV + C)}{(3X_c^{\,3})} - \frac{2}{V}\right\} \text{.....13}$$

$$R_P = R_P + R_{eq} \text{.....14}$$

$$R_P = \frac{r'_2}{s}(1-s) \text{.....15}$$

$$X_C = (aV^3 + bV^2 + cV + d)^{1/3} \text{.....16}$$

Similarly, for change in input wind power, the reactive power absorbed, $\Delta QPMIG$, in terms of generator terminal voltage, slip, and generator parameters can be written as

$$\Delta Q_{PMIG}(s) = K_6 \Delta P_{IW}(s) + K_7 \Delta V(s) \text{.....17}$$

Where

$$K_6 = \frac{-2X_{eq}R_T V^2}{(R_T^{\,2} + X_{eq}^{\,2})\{2R_T(P_{IW} - P_{coreloss}) + V^2\}} \text{.....18}$$

$$K_7 = \left[K_{C1} + \frac{V^2}{X_C}\left\{\left(\frac{3aV^2 + 2bV + c)}{(3X_C^{\,3})}\right) - \frac{2}{V}\right\}\right] \text{.....19}$$

Where

©IJRASET 2015: All Rights are Reserved

$$K_{C1} = \frac{-2X_{eq}V}{R_Y{}^2 + X_{eq}{}^2}\left[1 + \frac{2R_Y R_P V^2}{(R_y{}^2 + X_{eq}{}^2)\{2R_Y(P_{1W} - P_{coreloss}) + V^2\}}\right] \quad \text{.....20}$$

If *XC* is infinite, then PMIG behaves like an IG.

Finally, in (3), the term left is $\Delta Q\text{com}(s)$ i.e., the deviation in STATCOM reactive power, which can be expressed in terms of system state variables as given hereinafter. The STATCOM is based on a solid-state synchronous voltage source that is analogous to an ideal synchronous machine which generates a balanced set of three sinusoidal voltages, at the fundamental frequency, with rapidly controllable amplitude and phase angle. It consists of a VSC, a coupling transformer, and a dc capacitor as shown in Fig. 5.6. The real current of the STATCOM is negligible and is assumed to be zero. Control of reactive current is possible by variation of δ and α as shown in Fig. 5.7. Here, δ is the phase angle of the system bus voltage *V* where STATCOM is connected, and α is the angle of the fundamental output voltage *kV*dc of the STATCOM. The magnitude of the fundamental component of the converter output voltage is *kV*dc, where *V*dc represents the voltage across the capacitor. The reactive power injection to the system bus has the form

$$Q_{COM} = KV^2{}_{dc}B - KV_{dc}VB\cos(\alpha - \partial) + KV_{dc}VG\sin(\alpha - \partial) \text{.....21}$$

The system bus voltage *V* is taken as the reference voltage, and therefore, the angle δ is zero. Also, *G* is negligible as *G* + *jB* represents the step-down transformer admittance. Therefore, considering the value of *G* and δ to be zero, (21) can be written as

$$Q_{com} = KV^2{}_{dc}B - KV_{dc}VB\cos\alpha \text{.....22}$$

The flow of reactive power depends upon the variables *V* and α, and therefore, for small perturbation, the linearized STATCOM equation can be

$$\Delta Q_{com}(s) = K_8\Delta\alpha(S) + K_9\Delta V(s) \text{..... 23}$$

Where

$$K_{10} = KV_{dc}VB\sin\alpha \text{.....24}$$

$$K_{11} = -KV_{dc}B\cos\alpha \text{.....25}$$

Using these equations, a simulation model of the system has been developed, and the transfer function block diagram of the system is shown in Fig. 5.5. The transfer function block with *K*5
is replaced by the transfer function block shown by dotted lines when change in input wind power is considered.

III. TRANSIENT PERFOMANCE OF THE SYSTEM

The simulation results of three examples of the hybrid systems $W - D1$, $W - D2$, and $W - D3$ are given in this section for the typical data given in Table 6.1 and 6.2. The optimum gain values of the STATCOM controller using the ISE criterion have been obtained as given in Table 5.1. It has been observed that the decrease in STATCOM size with the decrease in wind power generation in the hybrid power system may require higher gain values to offset the mismatch of reactive power under transient conditions.

The transient responses of the systems $W - D_1$, $W - D_2$, and $W - D_3$ when wind energy conversion system (WECS) uses IG for 1% step increase in load, ΔQ_L , and no change in input wind power are shown in Fig. 6. It has been observed that the peak value of the voltage deviation increases as the size of the wind turbine increases. The increase in reactive power load has been supplied by the compensator under steady- state conditions as shown in Fig. 6(d). The transient responses of the systems $W - D_1$, $W - D_2$, and $W - D_3$ when WECS uses PMIG for 1% step increase in load, ΔQ_L , and no change in input wind power are shown in Fig. 7. Here, it has been observed that the peak value of the voltage deviation increases as the size of the wind turbine with PMIG reduces.

The transient responses of the systems $W - D_1$, $W - D_2$, and $W - D_3$ when WECS uses IG for 1% step increase in load, ΔQ_L , plus 1% step increase in input wind power, ΔP_{IW} , are shown in Fig. 8. The increase in input wind power also increases the

©IJRASET 2015: All Rights are Reserved

Volume 3 Issue VI, June 2015
ISSN: 2321-9653
International Journal for Research in Applied Science & Engineering Technology (IJRASET)

reactive power demand of the IG, and therefore, fluctuations are more compared to Fig. 6, but the settling time of the responses remains the same due to the fast action of the STATCOM in controlling the deviations. The transient responses of the systems $W-D_1$, $W-D_2$, and $W-D_3$ when WECS uses PMIG for 1% step increase in reactive load, ΔQ_L, plus 1% step increase in input wind power, ΔP_{IW}, are shown in Fig. 9

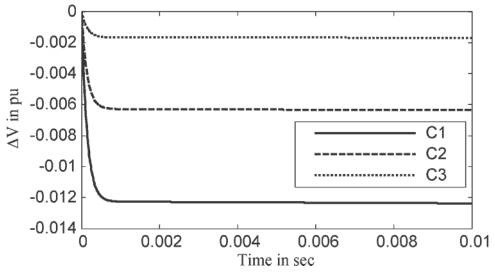

Fig. 8. Transient responses for voltage deviations of W-D1 system without STATCOM when WECS uses PMIG for step load disturbances of (C1) 10%, (C2) 5%, and (C3) 1%.

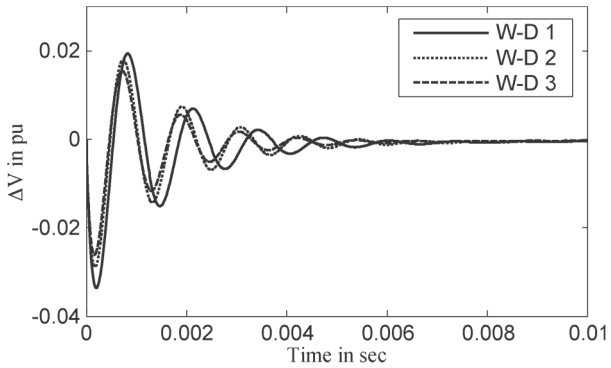

Fig. 9. Transient responses for voltage deviations of W-D1, W-D2, and W-D3 with STATCOM when WECS uses PMIG for 50% step load disturbances

It has been observed that, with wind input disturbances, the voltage deviations have similar trend as in the case of IG. However, it has more fluctuations in ΔQ_{PMIG} as compared to ΔQ_{IG}. During transient condition, both the SG and STATCOM provide the reactive power, but under steady-state condition, only STATCOM meets the reactive power demand of the system.

W-D1			W-D2		W-D3	
Constants	IG	PMIG	IG	PMIG	IG	PMIG
K1	0.15	0.15	0.15	0.15	0.15	0.15
K2	0.7392	0.7932	0.7590	0.7590	0.6737	0.67374
K3	6.22178	6.221	5.9531	5.95319	5.2842	5.2842
K4	-7.8249	-7.824	-9.6627	-9.6627	-8.082	-8.082
K5	0.1016	-0.666	0.0861	-0.6815	0.056	-0.7116
K6	0.444	-0.444	0.4535	0.4535	0.3034	0.3034
K7	-0.0974	-0.865	-0.0828	-0.8505	-0.0427	-0.8103
K10	5.15286	3.36	4.59882	3.10	3.56058	2.5727
K11	-3.8347	-2.5	- 3.4260	2.3099	-2.6522	-1.9114
KV	0.6667	0.667	0.6667	0.667	0.6667	0.667
TV	5.43E-04	5.43E-04	5.43E-04	5.43E-04	5.43E-04	5.43E-04

©IJRASET 2015: All Rights are Reserved

Volume 3 Issue VI, June 2015
ISSN: 2321-9653
International Journal for Research in Applied Science & Engineering Technology (IJRASET)

Table 6.1 Values of constants W-D1, W-D2, W-D3

System Parameters	W-D1	W-D2	W-D3
Wind capacity (kw)	1500	1500	1500
Diesel capacity (kw)	1500	1500	1500
Load capacity (kw)	2500	2500	2500
Base power (kw)	2500	2500	2500
IG			
$P_{IG}(p.u)$	0.6	0.5	0.333
$Q_{IG}(p.u)$	0.2906	0. 242161	0.161
η (%)	90	90	90
$r_1 = r_2^{'}(p.u)$	0.19	0.228	0.25
$x_1 = x_2^{'}(p.u)$	0.56	0.685	0.74
S(%)	-4	-4	-3
$T^{'}_{do}(\sec)$	5	5	5
X_d (p.u)	1	1	1
$X_d^{'}$ (p.u)	0.15	0.15	0.15
∂ (degree)	21.05	26.75	37.567
$E^{'}_q$	0.9603	0.92564	0.838
E_q	1.1136	1.1108	1.094
PMIG			
$P_{PMIG}(p.u)$	0.6	0.5	0.333
$Q_{PMIG}(p.u)$	0	0	0
$\eta(\%)$	90	90	90
$r_1 = r'_2$	0.19	0.228	0.25
$x_1 = x'_2$	0.56	0.685	0.74
$s(\%)$	-4	-4	-3
SG			
$P_{SG}(p.u)$	0.4	0.4	0.4
$Q_{SG}(p.u)$	0.2	0.2	0.2
STATCOM			
$T_1(ms)$	10-50	10-50	10-50
$T_\alpha(ms)$	0.2-0.3	0.2-0.3	0.2-0.3
$T_d(ms)$	1.67	1.67	1.67

©IJRASET 2015: All Rights are Reserved

IEEE type -1 system K_A, K_E K_F, T_A(sec) S_F, T_E(sec)	40,1.0 0.5,0.05 0, 0.55	40,1.0 0.5,0.05 0, 0.55	40,1.0 0.5,0.05 0, 0.55

Table 6.2 Values of constant /parameters W-D1,W-D2,W-D3

Further tests have been conducted on the system for 5% and 10% reactive load disturbances as shown in Fig. 10. It has been observed that the first peak of voltage deviation increases, but the settling time remains the same as less than 0.01 s. The transient study for voltage deviations of the W-D1 system when WECS uses PMIG without STATCOM has been carried out for different step load changes as shown in Fig. 11. It has been observed that the variations are large and the automatic voltage regulator (AVR) with SG is not able to maintain the voltage at the desired level. Therefore, STATCOM is necessary to eliminate the reactive power mis- match, and its fast action stabilizes the responses in less than 0.01 s irrespective of the size of the disturbance. The transient responses for the voltage deviations of the W-D1, W-D2, and W-D3 for 50% step increase in the reactive power load are shown in Fig. 12.

IV. CONCLUSION

Reactive power control of isolated wind–diesel hybrid power systems has been investigated when WECS uses PMIG for power generation. The WECSs are interconnected to diesel generation-based grid for the enhancement of capacity and fuel saving. The system also comprises STATCOM for reactive power support during steady-state and transient conditions. A mathematical model of the system has been derived for investigating the dynamic performance of the system. For comparison of performance with the existing systems, WECS has also been considered with IG for power generation. Three examples of wind–diesel systems with different wind power generation capacities have been considered for study. It has been observed that the STATCOM effectively stabilizes the oscillations in less than 0.01 s, caused by disturbances in reactive power load and in input wind power. As steady-state condition is reached, the STATCOM provides the additional reactive power required by the system. It has also been observed that, as the unit size of the wind-power generation decreases, the value of the optimum gain setting increases. The W-D systems with PMIG have the added advantage of reduction in the size of the STATCOM but have comparable transient performance when W-D system uses IG for power generation. The PMIG also has higher efficiency than the IG. Therefore, PMIGs are very good options for W-D systems than IG.

REFERENCES

[1] J. K. Kaldellis, Stand-Alone and Hybrid Wind Energy Systems: Technology, Energy Storage and Applications. Cambridge, U.K.: Woodhead Publ. Ltd., 2011.
[2] R. Hunter and G. Elliot, Wind–Diesel Systems, A Guide to the Technology and Its Implementation. Cambridge, U.K.: Cambridge Univ. Press, 1994.
[3] H. Nacfaire, Wind–Diesel and Wind Autonomous Energy Systems. London, U.K.: Elsevier Appl. Sci., 1989.
[4] T. K. Saha and D. Kastha, "Design optimization and dynamic performance analysis of a standalone hybrid wind diesel electrical power generation system," IEEE Trans. Energy Convers., vol. 25, no. 4, pp. 1209–1217,Dec. 2010.
[5] R. Pena, R. Cardenas, J. Proboste, J. Clare, and G. Asher, "Wind–diesel generation using doubly fed induction machines," IEEE Trans. Energy Convers., vol. 23, no. 1, pp. 202–214, Mar. 2008.
[6] R. Cardenas, R. Pena, M. Perez, J. Clare, G. Asher, and F. Vargas, "Vector control of front end converters for variable speed wind diesel systems,"IEEE Trans. Ind. Electron., vol. 53, no. 4, pp. 1127–1136, Jun. 2006.
[7] S. Roy, "Reduction of voltage dynamics in isolated wind–diesel units susceptible to gusting," IEEE Trans. Sustainable Energy, vol. 1, no. 2, pp. 84–91, Jul. 2010.
[8] A. M. Kaseem and A. M. Yousf, "Robust control of an isolated hybrid wind–diesel power system using linear quadratic Gaussian approach," Elect. Power Energy Syst., vol. 33, no. 4, pp. 1092–1100, 2011.
[9] R. C. Bansal, "Automatic reactive power control of isolated wind–diesel hybrid power systems," IEEE Trans. Ind. Electron., vol. 53, no. 4, pp. 1116–1126, Jun. 2006.
[10] C. Abbey,W. Li, and G. Joos, "An online control algorithm for application of a hybrid ESS to a wind–diesel system," IEEE Trans. Ind. Electron., vol. 57, no. 12, pp. 3896–3904, Dec. 2010.
[11] M. Liserre, R. Cardenas, M. Molinas, and J. Rodríguez, "Overview of multi-MW wind turbines and wind parks," IEEE Trans. Ind. Electron.,vol. 58, no. 4, pp. 1081–1095, Apr. 2011.
[12] T. Zhou and B. Francois, "Energy management and power control of a hybrid active wind generator for distributed power generation and gridintegration," IEEE Trans. Ind. Electron., vol. 58, no. 1, pp. 95–104,Jan. 2011.
[13] T. Fukami, K. Nakagawa, Y. Kanamaru, and T. Miyamoto, "A technique for the steady-state analysis of a grid-connected permanent-magnet induction generator," IEEE Trans. Energy Convers., vol. 19, no. 2, pp. 318–324,Jun. 2004.

©IJRASET 2015: All Rights are Reserved

[14] T. Fukami, K. Nakagawa, Y. Kanamaru, and T. Miyamoto, "Performance analysis of the permanent-magnet induction generator under unbalanced grid voltages," Denki Gakkai Ronbunshi, vol. 126, pp. 1126–1133, 2006.
[15] J. F. H. Douglas, "Characteristics of induction motors with permanentmagnet excitation," AIEE Trans. Power App. Syst., vol. 78, no. 3, pp. 221– 225, Apr. 1959.
[16] B. Ackermann, "Single phase induction motor with permanent-magnet excitation," IEEE Trans. Magn., vol. 36, no. 5, pp. 3530–3532, Sep. 2000.
[17] T. Fukami, K. Nakagawa, Y. Kanamaru, and T. Miyamoto, "Effects of the built-in permanent magnet rotor on the equivalent circuit parameters of a permanent magnet induction generator," IEEE Trans. Energy Convers., vol. 22, no. 3, pp. 798–799, Sep. 2007.
[18] T. Fukami, K. Nakagawa, R. Hanaoka, S. Takata, and T. Miyamoto, "Nonlinear modeling of a permanent-magnet induction machine," Trans. Inst. Elect. Eng. Jpn., vol. 122-D, no. 7, pp. 752–759, Jul. 2002.
[19] P. Sharma, T. S. Bhatti, and K. S. S. Ramakrishna, "Study of an isolated wind–diesel hybrid power system with STATCOM by incorporating a new mathematical model of PMIG," Eur. Trans. Elect. Power, DOI: 10.1002/etep.566, to be published.
[20] J. H. J. Potgieter, A. N. Lombard, R. J. Wang, and M. J. Kamper, Evaluation of Permanent-Magnet Excited Induction Generator for Renewable Energy Applications. [Online]. Available: research.ee.sun.ac.za/emr/ files/u1/Paper29JHJPotgieter.pdf
[21] N. G. Hingorani and L. Gyugyi, Understanding FACTS: Concepts and Technology of Flexible AC Transmission Systems. New York: IEEE Power Eng. Soc., 2000.
[22] Y. H. Song and A. T. Johns, Flexible A. C. transmission Systems (FACTS), IEE Power and Energy Series 30. London, U.K.: Inst. Elect. Eng., 1998.
[23] B. Kouadri and Y. Tahir, "Power flow and transient stability modeling of a 12-pulse statcom," J. Cybern. Inform., vol. 7, pp. 9–25, 2008.
[24] A. Yazdani, H. Sepahvand, M. L. Crow, and M. Ferdowsi, "Fault detectionand mitigation in multi-level converter STATCOMs," IEEE Trans. Ind. Electron., vol. 58, no. 4, pp. 1307–1315, Apr. 2011.

©IJRASET 2015: All Rights are Reserved

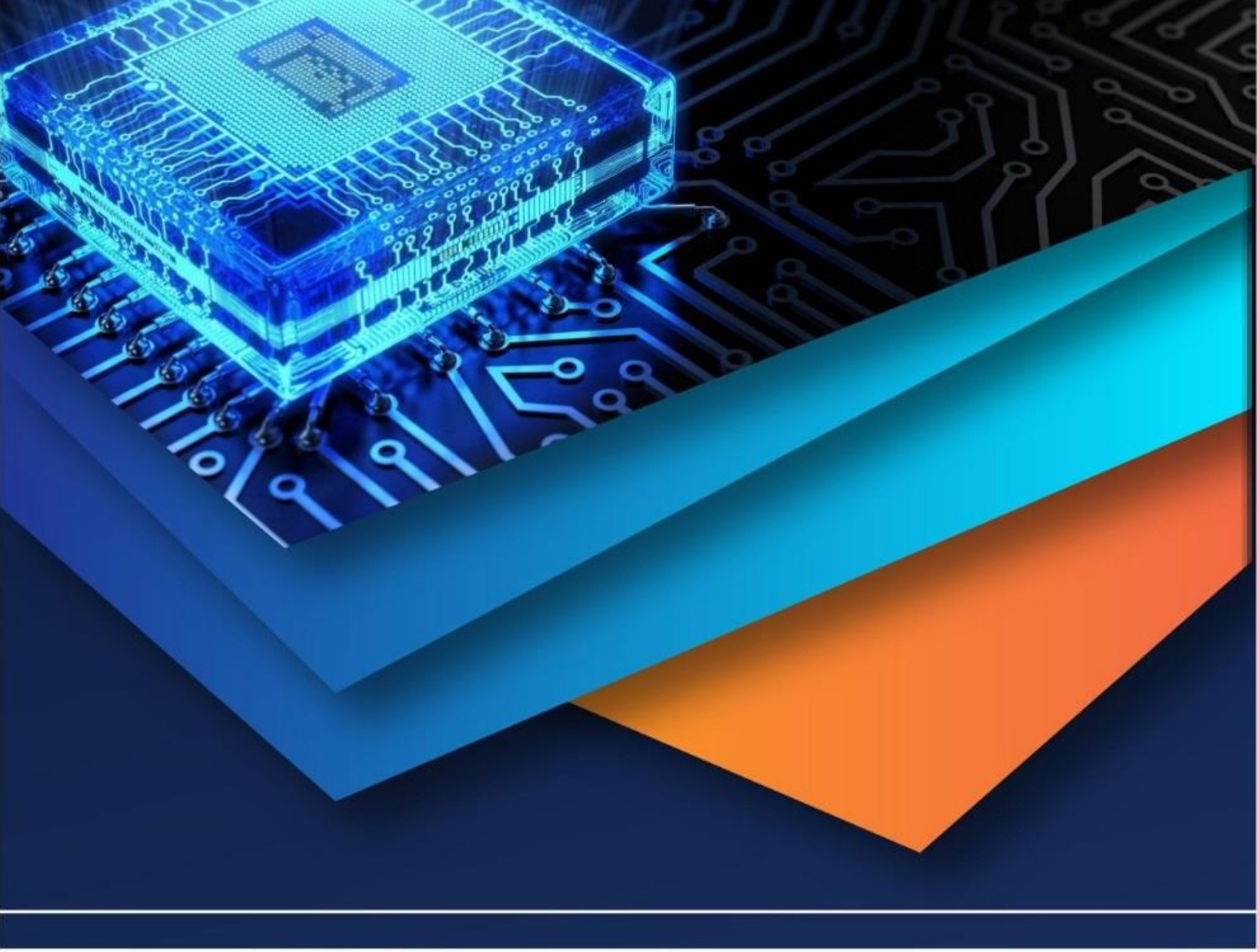

10.22214/IJRASET

45.98

IMPACT FACTOR: 7.129

IMPACT FACTOR: 7.429

INTERNATIONAL JOURNAL FOR RESEARCH

IN APPLIED SCIENCE & ENGINEERING TECHNOLOGY

Call : 08813907089 (24*7 Support on Whatsapp)